Volume loss in shallow tunnelling

Vu, M.N.; Broere, Wout; Bosch, Johan

Publication date
2016

Document Version
Accepted author manuscript

Published in
Tunnelling and Underground Space Technology

Citation (APA)
Vu, M. N., Broere, W., & Bosch, J. (2016). Volume loss in shallow tunnelling. *Tunnelling and Underground Space Technology*, *59*, 77-90. http://10.1016/j.tust.2016.06.011

Volume loss in shallow tunnelling

Minh Ngan Vu[a,b,*], Wout Broere[a], Johan Bosch[a]

[a] *Delft University of Technology, Geo-Engineering Section, Stevinweg 1, 2628 CN Delft, the Netherlands*
[b] *Hanoi University of Mining and Geology, Faculty of Civil Engineering, Vietnam*

Abstract

Although volume loss has an important effect in estimating the ground movements due to tunnelling in the design stage, this parameter is often determined by experience. This makes it difficult to estimate the impact on volume loss when changing project parameters like soil conditions, depth of the tunnel or sensitivity of the surroundings. This paper investigates the relationship between volume loss and cover-to-diameter C/D ratio in shallow tunnelling. Based on a number of (empirical) relations from literature, such as the stability number method and an analysis of the bentonite and grout flows, volume loss at the face, along the shield and at the tail is determined. Long-term volume loss behind the shield is also estimated by means of consolidation. In this way a band width of achievable volume loss for future projects is derived.

Keywords: cover-to-diameter ratio; volume loss; TBM; tail void; shallow bored tunnel

1. Introduction

Tunnelling often leads to settlements of the soil surface due to over-excavation, soil relaxation and inefficient tail void filling. The magnitude of volume loss is influenced by tunnelling management, characteristics of the tunnel boring machines (TBM), and the geotechnical conditions. In predictions of surface settlement (Peck, 1969) and subsurface settlement (Mair et al., 1993), the volume loss is often determined by engineering experience

*Corresponding author: Tel.:+31 15 278 1930; Fax:+31 15 278 1189
Email address: N.Vuminh@tudelft.nl/vuminhngan@gmail.com (Minh Ngan Vu)

and data from previous cases. This makes it difficult to correctly assess the volume loss for a future project under radically different conditions like a shallow depth of the tunnel and/or very different soil parameters. A ground movement analysis in Vu et al. (2015a) shows the important role of volume loss for settlement calculations and in predicting the effects on existing buildings induced by tunnelling. Especially for (very) shallow tunnels near building foundations, the impact of changes in volume loss is large. Most previous studies on volume loss start from a given volume loss and establish deformation patterns from that or correlate surface observations to volume loss at the tunnel for specific projects. Mair et al. (1982); Attewell et al. (1986); Macklin (1999); Dimmock and Mair (2007) studied the volume loss with a summary of projects in overconsolidated clay relating to the volume loss at the tunnelling face. Verruijt and Booker (1996); Verruijt (1997); Strack (2002) applied analytical methods for predicting the ground loss around the tunnel. Loganathan (2011) proposed volume loss calculations but only approximated volume loss along the shield with the worst case, and does not take the consolidation into account. Meanwhile, Bezuijen and Talmon (2008) showed the effect of grouting pressure on the volume loss around the TBM but none of these includes a detailed method to estimate volume loss along the TBM. This paper aims to estimate the volume loss when tunnelling with limited C/D ratios (i.e. less than 1) in various soils with a focus on slurry shield tunnelling.

On the basis of the studies by Attewell and Farmer (1974), Cording and Hansmire (1975) and Mair and Taylor (1999), the volume loss in the tunnelling progress can be estimated by the sum of the following components as shown in Figure 1:

- Volume loss at the tunnelling face: soil movement towards the excavation chamber as a result of movement and relaxation ahead of the face, depending on the applied support pressures at the tunnelling face;
- Volume loss along the shield: the radial ground loss around the tunnel shield due to the moving soil into the gap between the shield and surrounding soil, which can be caused by overcutting and shield shape. The bentonite used in the tunnelling face flows into the gap, while the grout used in the shield tail also flows in the opposite direction. Due to the drop of bentonite and grout flow pressures in a constrained gap, soil can still move into the cavity when the soil pressure is larger than the bentonite pressure or grout pressure;
- Volume loss at the tail: when precast segments are placed, the advance of the shield results an annular cavity between the segments and surrounding

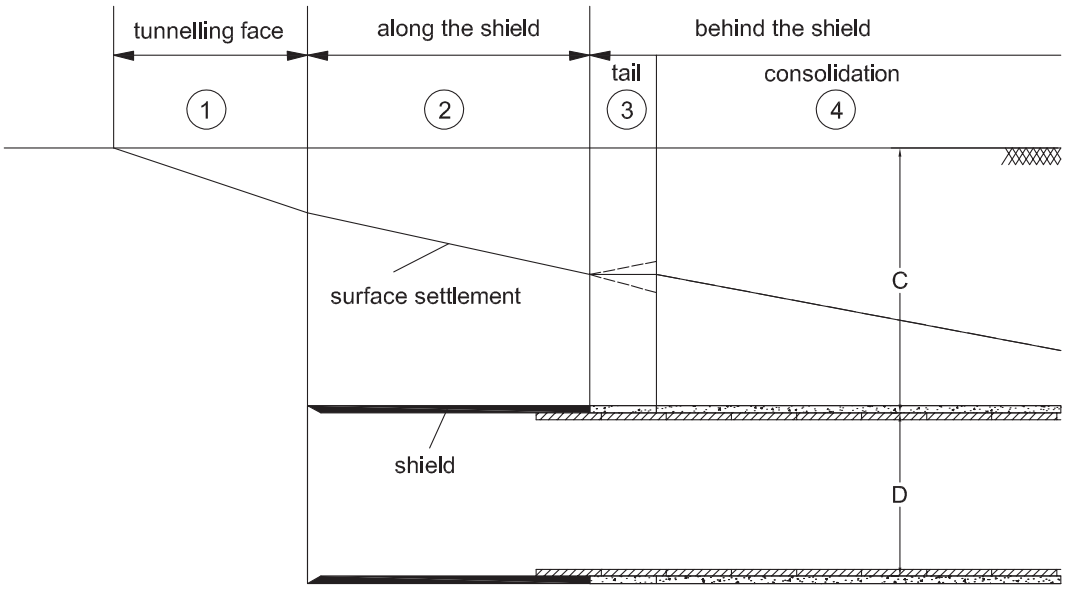

Figure 1: Volume loss components

soil. Grout is used in order to prevent surrounding soil moving into the gap. Volume loss at the tail depends on applied grouting pressure at the tail and proper volume control, where high grout volume and pressure may lead to local heave and low volume to increase settlements as indicated in Figure 1;
- Volume loss behind the shield tail due to consolidation: in this void along the tunnel lining, grout consolidates and forms a grout cake, and the stress changes induced in the soil may lead to long-term consolidation settlements in soil volume above the tunnel. Other causes of volume loss are shrinkage of grout and long-term lining deformations. However, their contributions to the total volume loss are small comparing to the above factors.
The total volume loss V_L in tunnelling progress can be given as:

$$V_L = V_{L,f} + V_{L,s} + V_{L,t} + V_{L,c} \tag{1}$$

where $V_{L,f}$ is volume loss at the tunnelling face, $V_{L,s}$ is volume loss along the shield, $V_{L,t}$ is volume loss at the tail, and $V_{L,c}$ is volume loss due to consolidation.

To illustrate the impact of the different contributions in different soil conditions, estimates are made for a number of ideal soil profiles which are derived from Amsterdam North-South metro line project (Gemeente-Amsterdam,

2009), consisting of a single soil type with most important properties as defined in Table 1, where γ is volumetric weight, φ is the friction angle, K is the initial coefficient of lateral earth pressure, c is cohesion, C_s is compression constant, C_{swel} is swelling constant, ν is Poisson's ratio and E_s is the stiffness modulus of the ground.

Table 1: Soil parameters used in design of Amsterdam North-South metro line project (Bosch and Broere, 2009; Gemeente-Amsterdam, 2009)

Soil type	$\gamma(kN/m^3)$	$\varphi(^o)$	$K(-)$	$c(kN/m^2)$	$C_s(-)$	$C_{swel}(-)$	$\nu(-)$	$E_s(kN/m^2)$
Sand	20	35	0.5	-	-	-	0.2	20000
Clayey sand	17.9	35	0.4	2	-	-	0.2	12000
Clay	16.5	33	0.5	7	100	1000	0.15	10000
Organic clay	15.5	20	0.65	5	80	800	0.15	5000
Peat	10.5	20	0.65	5	25	250	0.15	2000

2. Volume loss at the tunnelling face

When tunnelling, the soil ahead of the excavation chamber generally has the trend to move into the cavity which is created by the tunnelling machine. The soil volume moving towards the face depends on applied support pressures and can be controlled by adjusting the support pressures. In stability analysis for tunnelling, the stability number N proposed by Broms and Bennermark (1967) is widely used. By studying the relationship between this stability number and volume loss at tunnelling face, Attewell et al. (1986), Mair et al. (1982), Mair (1989), Macklin (1999) and Dimmock and Mair (2007) presented a method to determine the expected volume loss based on observed data.
The stability number N is given by:

$$N = \frac{\gamma\,(C + D/2) - s}{c_u} \tag{2}$$

where s is the support pressure at the tunnelling face and c_u is undrained shear strength of the soil.
In shallow tunnelling, the support pressure at the tunnelling face should be high enough to avoid the collapse to the excavation chamber but also limited to prevent blow-out and fracturing. Firstly, the required support

pressure must be higher than or at least equal to the total of water pressure and horizontal effective soil pressure taking into account three dimensional arching effects. The wedge model, which was studied by Anagnostou and Kovári (1994), Jancsecz and Steiner (1994) and Broere (2001), is commonly applied to determine the minimum support pressure s_{min}. In the case of shallow tunnelling, the minimum support pressure s_{min} can be derived from the wedge model, as follows:

$$s_{min} = \sigma_h^{,} + p = \sigma_v^{,} K_{A3} + p = \gamma^{,} z K_{A3} + p \tag{3}$$

where p is pore pressure and K_{A3} is the three dimensional earth pressure coefficient determined in Jancsecz and Steiner (1994).
Secondly, the maximum support pressures are often estimated as to avoid blow-out and fracturing. According to Vu et al. (2015b), the maximum support pressures in the case of blow-out are given by:

$$s_{0,t,max} = \gamma \left(H - \frac{\pi}{8} D \right) + 2 \frac{H}{D} \left(c + \frac{1}{2} H K_y \gamma' tan\varphi \right) - \frac{aD}{4} \tag{4}$$

$$s_{0,b,max} = \gamma \left(H - \frac{\pi}{8} D \right) + 2 \frac{H}{D} \left(c + \frac{1}{2} H K_y \gamma' tan\varphi \right) + \gamma_T \pi d + \frac{aD}{4} \tag{5}$$

where $s_{0,t,max}$ and $s_{0,b,max}$ are the maximum support pressures at the top and bottom of the tunnel.
In normally consolidated soil, according to Mori et al. (1991), the maximum pressure in the case of fracturing is presented as:

$$s_f = \sigma_v^{,} K + p + c_u \tag{6}$$

However, field data show that the higher allowable support pressures are often applied in the tunnelling face, according to NEN-3650 (2012) and reports by BTL (Boren van Tunnels en Leidingen), in the Netherlands. Therefore, the support pressures boundaries are determined with the minimum support pressure and the maximum support pressure in the case of blow-out as indicated in Equations 4 and 5 above.
Figure 2 shows the relationship between the required support pressures and the C/D ratio with the tunnel diameter $D = 6m$ in clay. We will elaborate the calculation method for these conditions and present overall results for different diameters and soil conditions later in Figure 10. According to Vu et al. (2015b), only C/D ratios larger than 0.4 are studied, as less cover

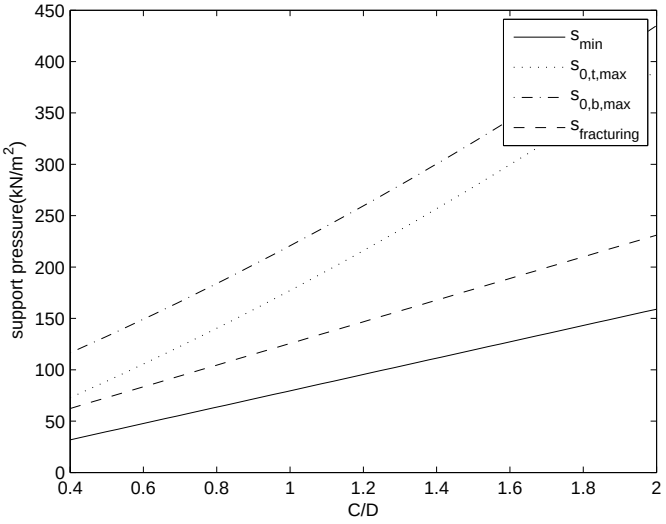

Figure 2: The range of support pressures at the tunnelling face of a tunnel with a diameter $D = 6m$ in clay

would lead to unreasonable large volume loss, and the upper 3 to 4 meter of soil in urban areas are often taken up by various utilities and therefore would not be available for tunnelling. The support pressures calculated here are the minimum support pressure from a wedge model and the maximum support pressures for fracturing and blow-out at the top and the bottom of the tunnel.

Figure 3 shows the calculated stability number N for these support pressures. Since the applied support pressures are derived from the wedge stability model, fracturing and blow-out conditions, N values in this figure are smaller than 2. It means that the tunnelling face is stable with these support pressures.

O'Reilly (1988) indicated that a relation exists between the volume loss at tunnelling face $V_{L,f}$ and the load factor LF, which is estimated by the ratio of working stability number N and the stability number at collapse N_{TC}, as follows:

$$LF = \frac{N}{N_{TC}} \tag{7}$$

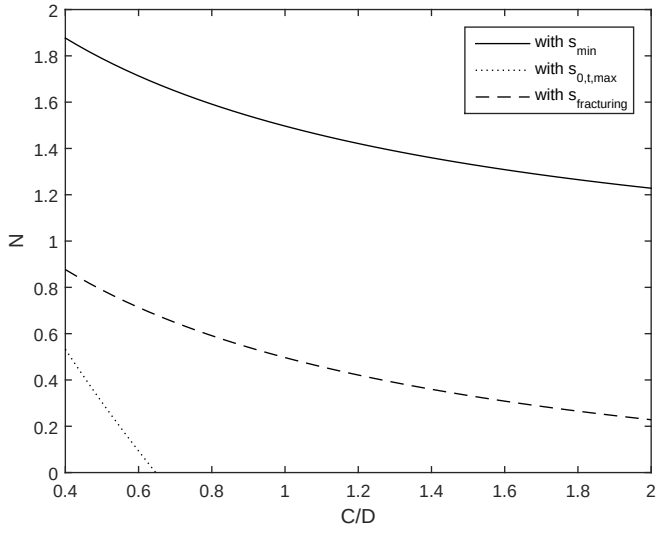

Figure 3: The range of stability number N for a tunnel with a diameter $D = 6m$ in clay

where N_{TC} is estimated according to Mair and Taylor (1999) as:
For $0 \leq C/D \leq 1$:

$$N_{TC} = 2 + 2ln\left(\frac{2C}{D} + 1\right)$$

For $1 \leq C/D \leq 1.8$:

$$N_{TC} = 4ln\left(\frac{2C}{D} + 1\right)$$

Figure 4 shows the relationship between the load factor LF and the C/D ratio. The load factor is less than 0.6 for the minimum support pressure and has the trend of reducing when the C/D ratio increases. This means that the tunnel becomes safer with regards to estimating the support pressures when the C/D ratio becomes larger.
From the analysis of case history data of the load factor LF and the volume loss at the tunnelling face (Figure 5), Macklin (1999) presented a formula to calculate the volume loss at the tunnelling face $V_{L,f}$ as:

$$V_{L,f}(\%) = 0.23e^{4.4LF} \tag{8}$$

Equation 8 can be used to convert the load factor LF to the volume loss $V_{L,f}$

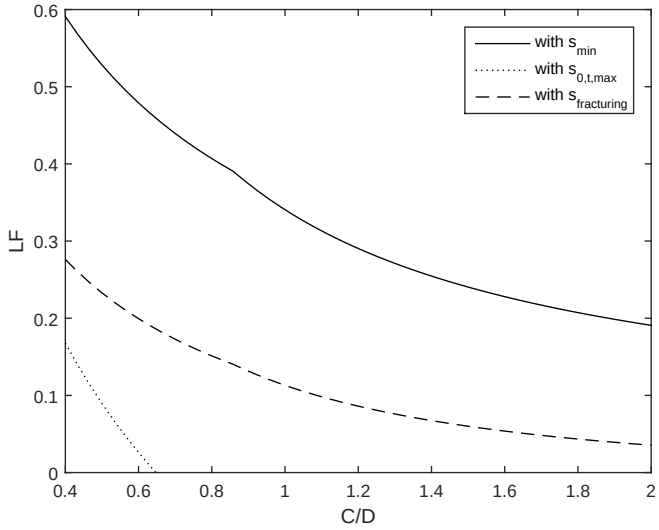

Figure 4: Relationship between load factor LF and C/D ratio for a tunnel with diameter D=6m in clay

estimates, which leads to Figure 6. This shows the range of volume loss at the tunnelling face $V_{L,f}$ with various C/D ratios for a tunnel with $D = 6m$ in clay. In shallow tunnels with $0.4 \leq C/D \leq 1$ the range of possible volume loss $V_{L,f}$ is large, ranging from 0.12% to 3.1%. This means that if tunnelling uses the minimum pressure in the excavation chambers, the volume loss $V_{L,f}$ will increase significantly. Meanwhile, the volume loss $V_{L,f}$ in the case of $1 \leq C/D \leq 2$ ranges from 0.27% to 1.05%. The difference in volume loss $V_{L,f}$ between the minimum pressure and maximum pressures due to blow-out and fracturing is clearly reduced. Therefore, in the case of very shallow tunnels ($C/D \leq 1$) the support pressures applied at the tunnelling face should be kept near to the maximum pressure in order to avoid increasing the volume loss.

3. Volume loss along the shield

The diameter of the cutting wheel in front of the TBM is often larger than the diameter of the shield. This leads to an overcut when tunnelling (Figure 7). Also, the TBM is often tapered, which creates a gap between

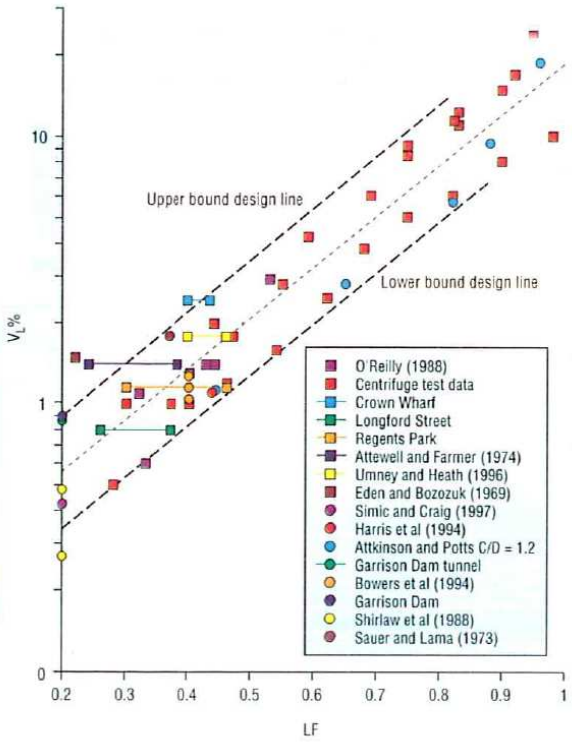

Figure 5: Volume loss $V_{L,f}$ and load factor LF (Macklin, 1999)

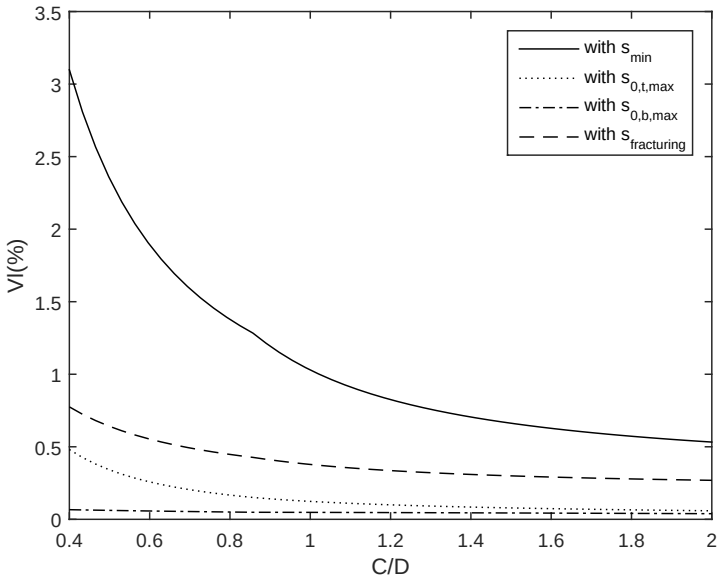

Figure 6: Volume loss at tunnelling face for a tunnel with diameter $D = 6m$ in clay

the shield skin and the surrounding soil. Additional gapping can also occur when the TBM moves in curves as indicated in Festa et al. (2015). In this study, the effect of curves is not included. This gap is often filled by bentonite, which flows from the tunnelling face and/or grout which comes from the shield tail. In practice, the grout and bentonite pressures are often larger than the vertical soil pressure at the tunnelling face and tail. From the observation of Bezuijen (2007), there are three possible bentonite and grout flows that can occur along the shield when tunnelling. Firstly, the bentonite flows from the tunnelling face to the tail and pushes the grout at the joint between the tail and the TBM. Secondly, the grout flows from the tail to the tunnelling face and pushes the bentonite away. Thirdly, the grout flows from the tail to the tunnelling face and the bentonite also flows in the opposite direction. The flows of bentonite and grout were also simulated in Nagel and Meschke (2011). In shallow tunnelling, due to the possibility of blow-out and fracturing, there is a limitation of applied grout and bentonite pressures at the tunnelling face and the tail.

According to Bezuijen (2007), both liquids, the grout in the shield tail and the bentonite applied at the tunnelling face are assumed to behave as the

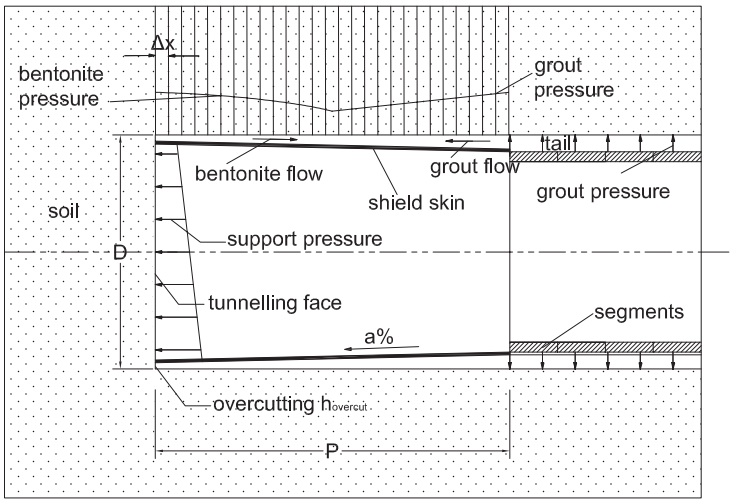

Figure 7: Bentonite and grout flows along the shield and lining segments

Table 2: Input parameters of tunnel boring machine

Diameter of shield D	$6m$
Length-to-diameter P/D ratio of the shield	1
Reduction of shield diameter a	0.2%
Overcutting $h_{overcut}$	$0.015m$
Shear strength of grout τ_y^{grout}	$1.6kPa$
Shear strength of bentonite $\tau_y^{bentonite}$	$0.8kPa$

Bingham liquids, such that the yield stress is governing in the flow behaviour. The flow pressures in grout and bentonite reduce along the shield as in Figure 7. The reduction of grout pressure along the shield is given by:

$$\Delta p = \frac{\Delta x}{w_j} \tau_y \tag{9}$$

where Δp is the change of the pressure due to flow, Δx is a length increment along the TBM, w_j is the joint width between the tunnel and the surrounding soil and τ_y is a shear strength of the grout around the TBM.
In this study, the volume loss along the shield is calculated with input parameters as indicated in Table 2 with the following approach.
As an example, the calculation is carried out with a case of tunnel with

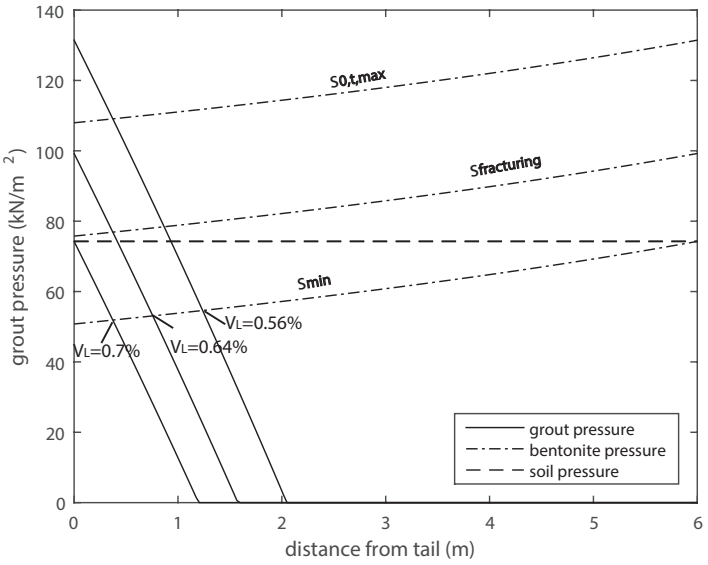

Figure 8: Bentonite and grout pressures along a shield with $D = 6m$ in clay

$D = 6m$ and $C/D = 0.75$ in clay. Figure 8 shows the change of grout pressure and bentonite pressure along the shield. It is assumed that when the grout pressure and bentonite pressure are less than the vertical soil pressure, the soil is moving into the cavity. The volume loss is estimated as the void volume that is filled by soil. The volume loss will not occur if the grout pressure and the bentonite pressure are larger than the vertical soil pressure. In that case, the gap along the shield is assumed to be completely filled by grout and bentonite. From this figure, the volume loss along the shield depends on the bentonite pressure, which is applied at the tunnelling face and the grout pressure at the tail. When the bentonite and grout pressures are equal to the minimum required pressure as calculated in previous section, the volume loss will be maximal. On the other hand, when the maximum allowable pressures are applied, there is no volume loss along the shield.
In order to investigate the effect of grout pressure on the shield in different soils, we assume the bentonite pressure applied at the tunnelling face is the average of the minimum support pressure and the maximum support pressure for fracturing. Figure 9 shows the change of volume loss with different tunnel diameters in various soils. When the C/D ratio increases, the range of

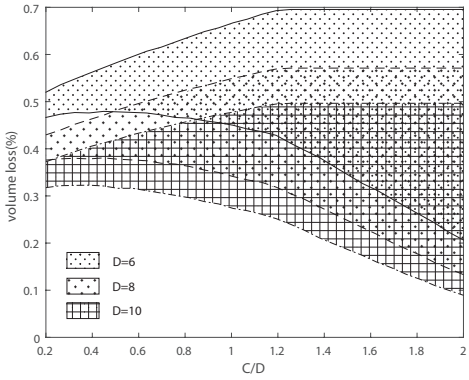

(a) in sand

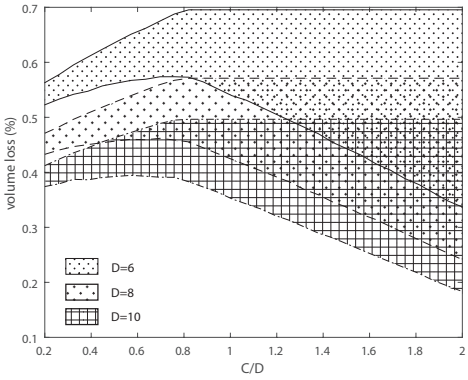

(b) in clayey sand

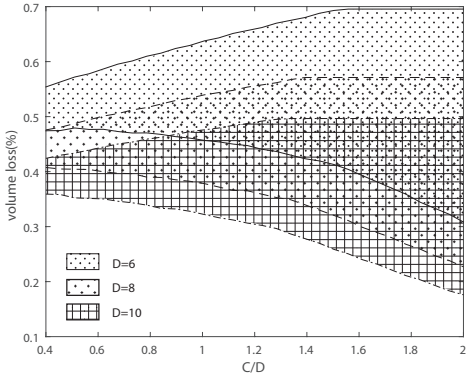

(c) in clay

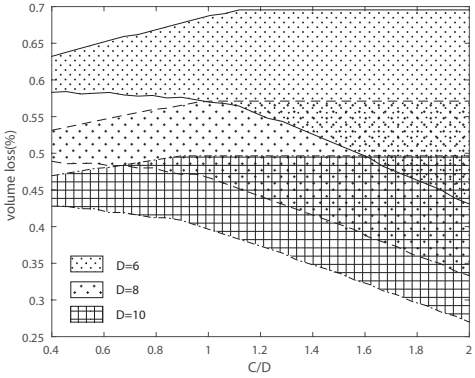

(d) in organic clay

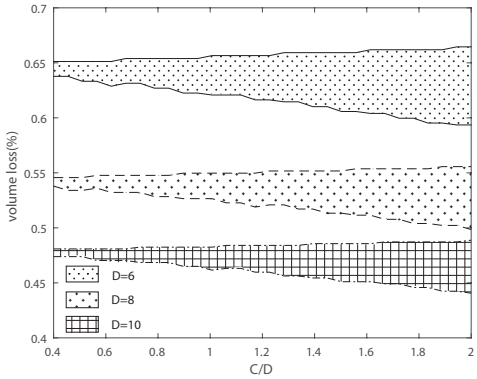

(e) in peat

Figure 9: Volume loss along the shield in various soils

the volume loss along the shield $V_{L,s}$ is larger. With a particular C/D ratio of the tunnel, the larger the tunnel diameter is, the smaller the volume loss $V_{L,s}$ is with the constant overcut parameter of the shield. In the case of tunnelling in sand, the upper boundary of the volume loss $V_{L,s}$ increases nearly linearly with the C/D ratio from 0.4 to 0.8, then becomes almost constant when the C/D ratio increases whereas the lower boundary reduces linearly when the C/D ratio increases. This also appears in the cases of tunnelling in clay and organic clay. At this point, basically, the entire annulus is filled by the surrounding soil, leading to a maximum attainable volume loss along the tail. In the case of tunnelling in peat, in the range of this analysis with $0.4 \leq C/D \leq 2$, the upper boundary of the volume loss $V_{L,s}$ lightly rises and the lower boundary linearly decreases. It is noted that the maximum upper boundary volume loss along the shield $V_{L,s}$ is the same for a given tunnel diameter. Regardless of soil conditions, for a tunnel with $D = 6m$, it follows that $V_{L,s,max} = 0.7\%$, with $D = 8m$, $V_{L,s,max} = 0.57\%$ and with $D = 10m$, $V_{L,s,max} = 0.5\%$.
Figure 10 shows the boundary of the volume loss along the shield $V_{L,s}$ in relationship with C/D ratios for different tunnel diameters in different soils. The upper boundary for $0.4 \leq C/D \leq 0.6$ corresponds to the case of tunnelling in peat in all three tunnel diameters. When tunnelling with $0.6 \leq C/D \leq 1$, the upper boundary is given by tunnelling in organic clay and when tunnelling with the C/D ratio larger than 1, the upper boundary becomes constant and depends on the tunnel diameter D. The maximum volume loss along the shield $V_{L,s}$ is about 0.7% for $D = 6m$, $V_{L,s,max} = 0.57\%$ for $D = 8m$ and $V_{L,s,max} = 0.5\%$ for $D = 10m$. For the lower boundary, there is a decreasing trend of the minimum volume loss along the shield $V_{L,s}$ when the C/D ratio increases. In the case of $D = 6m$ the maximum $V_{L,s}$ of the lower boundary is about 0.47% when $C/D = 0.5$. The maximum volume loss along the shield $V_{L,s}$ of the lower boundary is about 0.38% with $D = 8m$ and 0.32% with $D = 10m$ when $C/D = 0.5$. When $C/D = 2$, $V_{L,s,max} = 0.2\%$ for $D = 6m$, $V_{L,s,max} = 0.13\%$ for $D = 8m$ and $V_{L,s,max} = 0.09\%$ for $D = 10m$.

4. Volume loss behind the shield

When precast segments are placed, the advance of the shield results in an annular cavity between the segments and the surrounding soil due to the shape of the TBM and the overcut as discussed above. Grout is injected

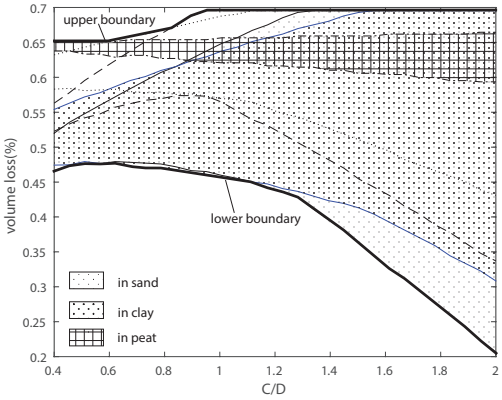

(a) $D = 6m$

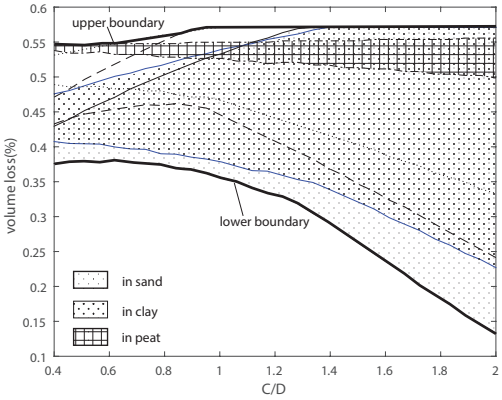

(b) $D = 8m$

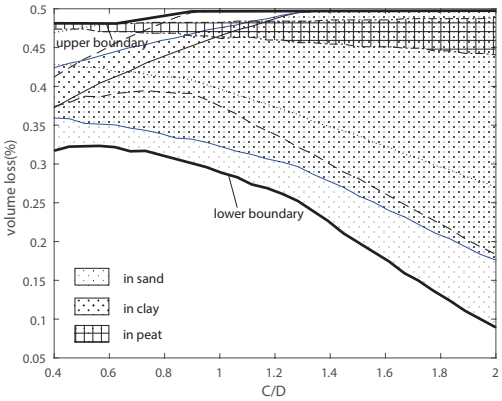

(c) $D = 10m$

Figure 10: Volume loss along the shield with different tunnel diameters

rapidly in order to prevent the surrounding soil to move into the gap. It is assumed that the void is filled by the grout. The injected grout pressure induces the loading on the soil around the tunnel lining. This might lead to immediate displacements and long-term consolidation of the soil. These are two components of the volume loss behind the shield: the volume loss at the tail and the volume loss due to consolidation.

4.1. Volume loss at the tail

When the grout is injected with high pressures at the tail, the ground around the tunnel will be deformed. In order to estimate the surface settlement induced by tunnelling, there are some analytical solutions proposed by Sagaseta (1988); Verruijt (1997); Strack (2002) based on cavity expansion and taking the influence of a free surface into account. However, the effect of the range of support pressures has not taken into account in these methods and resulting solutions, for instance expressed as a Laurent series expansion in the case of Verruijt (1997), require an increasing number of terms for a stable numerical integration if the distance between free surface and tunnel reduces. On the other hand, the cavity expansion developed for the case of a cavity in infinite medium has been implemented in tunnelling studies by Taylor (1993); Yu (2013) and results in far more elegant and practical solution for a first estimate of the effect of grout pressures on soil stresses and deformations around the TBM. To determine the effect of grouting at the tail on volume loss at the tail and consolidation, in this study, the cavity expansion method for tunnelling, which is proposed by Yu (2013), is therefore applied as a simplified method. In this cavity-expansion theory, it is assumed that the soil around the tunnel is a Tresca medium. The stresses in the soil and the settlement at the surface can be calculated by the cavity-expansion theory. According to Yu (2013), the plastic zone will deform around the tunnel wall, as can be seen in Figure 11, with the radius R_p of the plastic zone estimated from the following equation:

$$R_p = \frac{D}{2} \exp\left(\frac{\frac{p_0 - s}{Y} - \frac{k}{1+k}}{k} \right) \tag{10}$$

where p_0 is the pre-tunnelling pressure; $k = 1$ or 2 corresponding to cylindrical or spherical cavity models; $Y = 2c_u$ or $-2c_u$ corresponding to the case of contraction or expansion of the tunnel.

Similar to Yu (2013) and Taylor (1993), the pre-tunnelling pressure p_0 can be estimated as:

$$p_0 = \gamma \left(C + \frac{D}{2} \right) \tag{11}$$

The soil displacement u_s in the elastic zone is given by:

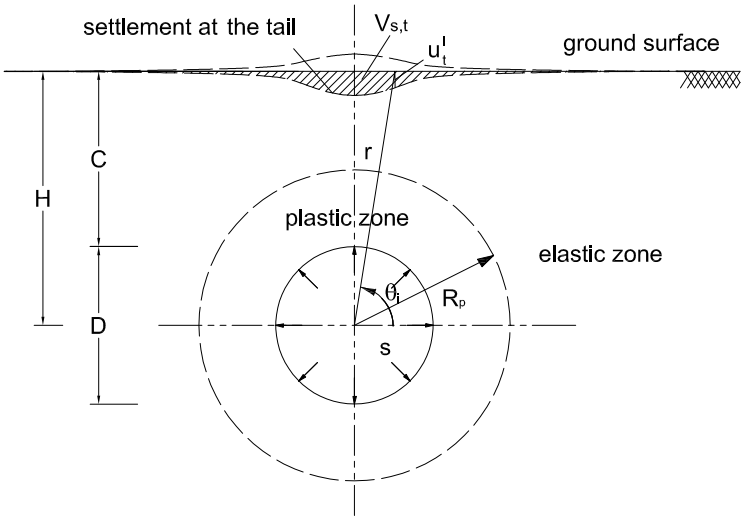

Figure 11: Deformations around a shallow tunnel at the tail

$$u_s = -\frac{Yr}{2(k+1)G} \left(\frac{R_p}{r} \right)^{1+k} \tag{12}$$

where r is the distance from the calculated point to the tunnel centre and $G = E/2(1+\nu)$ is the shear modulus of soil.
The soil displacement u_s in the plastic zone is given by:

$$u_s = -\frac{Y}{2(k+1)G} \left(\frac{D}{2r} \right)^k \frac{D}{2} \exp\left(\frac{(1+k)(p_0 - s)}{kY} - 1 \right) \tag{13}$$

In this case, the effect of grouting pressures at the tail is analysed with a cylindrical cavity model and is calculated with the minimum and maximum

support pressures. Thus, in Equation 10, k equals 1.
It can be assumed that the volume loss around the tunnel due to grouting at the tail equals the volume of ground settlement at the surface. In order to identify the contribution of soil deformation at the tail on the total volume loss, the displacement of the ground surface is estimated. According to assumptions in Yu (2013), the tunnel will collapse when the plastic zone expands to the ground surface. It means that when the tunnel is stable, the radial displacement of ground u_s at the surface is in the elastic zone and can be calculated with Equation 12.
The surface settlement at the tail can be estimated from:

$$u_t = u_s \sin\theta \tag{14}$$

where θ is the angle between the calculated point to the tunnel centre and the horizontal axis (see Figure 11).
The volume loss at the tail $V_{L,t}$ can be estimated as:

$$V_{L,t} = \frac{V_{s,t}}{\pi(D/2)^2} \tag{15}$$

where $V_{s,t}$ is the volume of the surface settlement due to grouting pressures at the tail (see Figure 11).
Figure 12 shows the boundaries of the volume loss at the tail $V_{L,t}$ in various soils for tunnels with $D = 6, 8$ and $10m$ with the range of the support pressures from the vertical soil stress to the maximum support pressure at the top of the tunnel derived from Equation 4. The figure shows that the larger the tunnel diameter is, the larger the range of volume loss $V_{L,t}$ is. When the support pressure equals the vertical soil stress at the top of the tunnel lining, there is a contraction in the cavity and this leads to positive values of the lower boundary of volume loss at the tail. When a high support pressure is used, the cavity will expand. The negative volume loss $V_{L,t}$ values indicate that the soil above the tunnel lining is pushed upward and there might be heave at the ground surface. In practice, this heave might not be observed because the settlement due to volume loss at the tunnelling face and along the shield could be larger. When a high support pressure is applied at the tail, a heave can occur in order to compensate the volume loss at the tunnelling face and along the TBM as can be seen in Figures 12a, 12b, 12c and 12d. However, in the case of very shallow tunnelling, there is no heave due to the small margin in the range of allowable support pressures as indicated in Vu

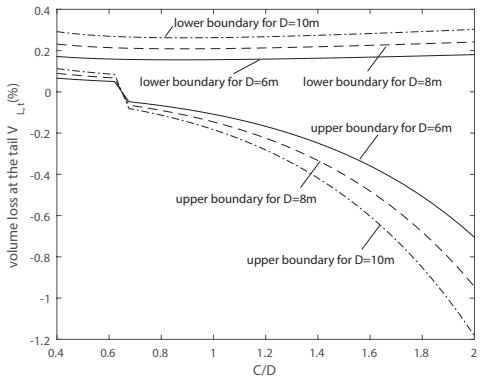

(a) in sand

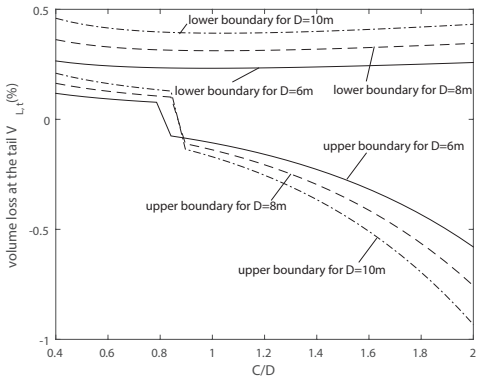

(b) in clayey sand

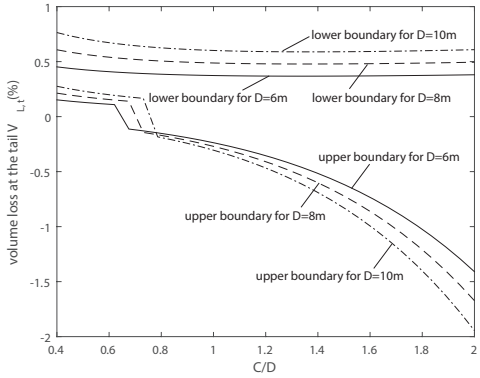

(c) in clay

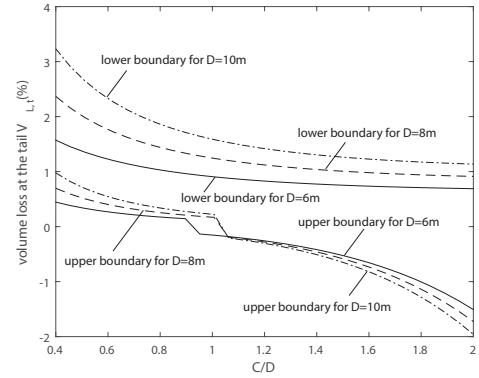

(d) in organic clay

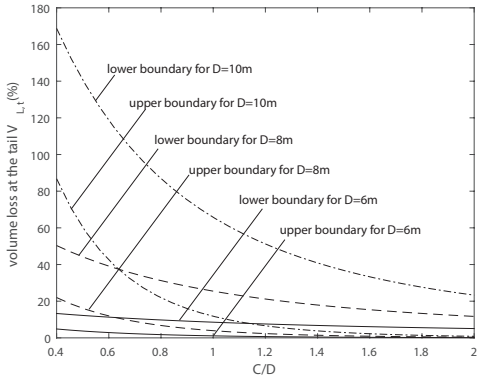

(e) in peat

Figure 12: Volume loss at the tail with different tunnel diameters in various soils

et al. (2015b). In Figure 12e, when tunnelling in peat, the volume loss at the tail is positive with a high value, especially in the case of a tunnel diameter $D = 10m$. It means that shallow tunnelling with a large diameter in peat might be difficult due to the large expected volume loss. This conclusion coincides with the conclusion indicated in Vu et al. (2015b) for the range of support pressure for shallow tunnelling in peat with low C/D ratios.
Figure 13 shows the dependence of $V_{L,t}$ values on soils in various tunnel diameters. When tunnelling in peat, the range of $V_{L,t}$ values is significantly large compared to tunnelling in sand, clay and organic clay, especially in the case of tunnels with large diameters as indicated above.

4.2. Volume loss due to consolidation

For the volume loss due to consolidation, in the cavity behind the tail, two consolidation processes occur along the tunnel lining. Firstly, the newly injected grout is consolidating and forms a consolidated grout cake in the cavity along the tunnel lining (Talmon and Bezuijen, 2009). In the case of tunnelling in clay, the consolidation in grout might not occur (Bezuijen and Talmon, 2013) and the length of liquid grout on the lining is much longer. Although the grout pressure decreases along the lining, the injected grout may flow along 2 to 3 following segments and the appearance of the grout cake will prevent the movement of the soil above. It is often assumed that there is no volume loss in the grout consolidating. The other volume loss is due to the subsequent shrinkage of grout, which is estimated at about 7 to 10 percent of total tail gap according to Loganathan (2011). However, the contribution of this volume loss to the total volume loss is small comparing to the other volume losses. This volume loss, therefore, is not taken into account in this study.
The second process is the consolidation of the soil volume above the tunnel behind the tail. When grout is applied at the tail, the soil stress in the above soil volume will change. This will induce consolidation in the long term behind the tail. The volume loss due to consolidation $V_{L,c}$ is derived from the consolidation settlement of the soil volume above tunnel lining. In the case of tunnelling in sand, consolidation of soil will probably not occur or be minimal. For tunnels in clay or peat, this may be a notable contribution. The consolidation settlement of the soil can be estimated from Terzaghi's formula, as follows:

$$u_c = -\frac{1}{C_s} \ln \left(\frac{\sigma_{soil}}{\sigma_0} \right) \tag{16}$$

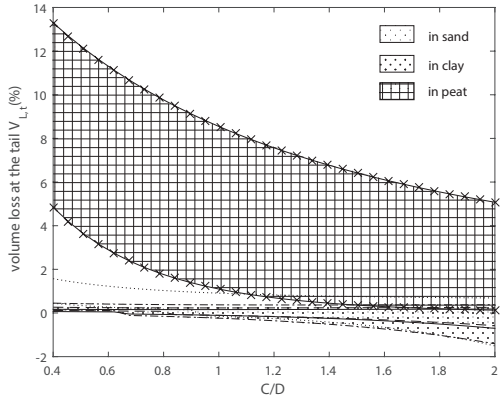

(a) $D = 6m$

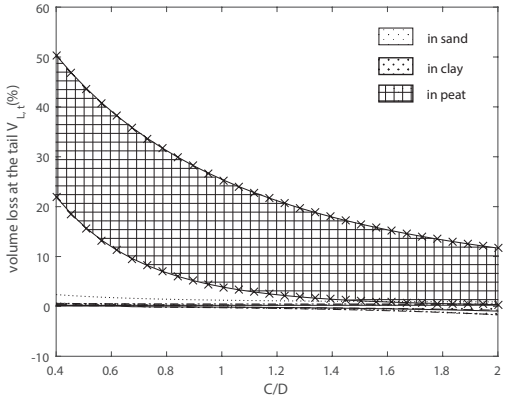

(b) $D = 8m$

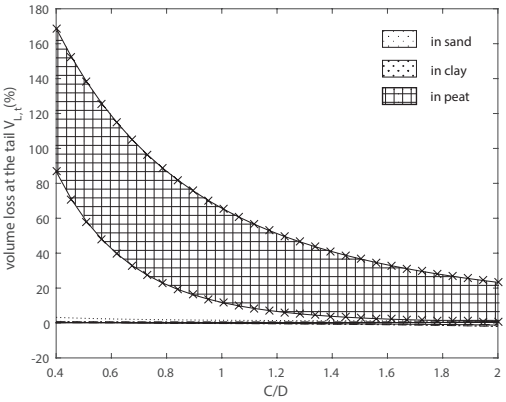

(c) $D = 10m$

Figure 13: Volume loss at the tail with different tunnel diameters

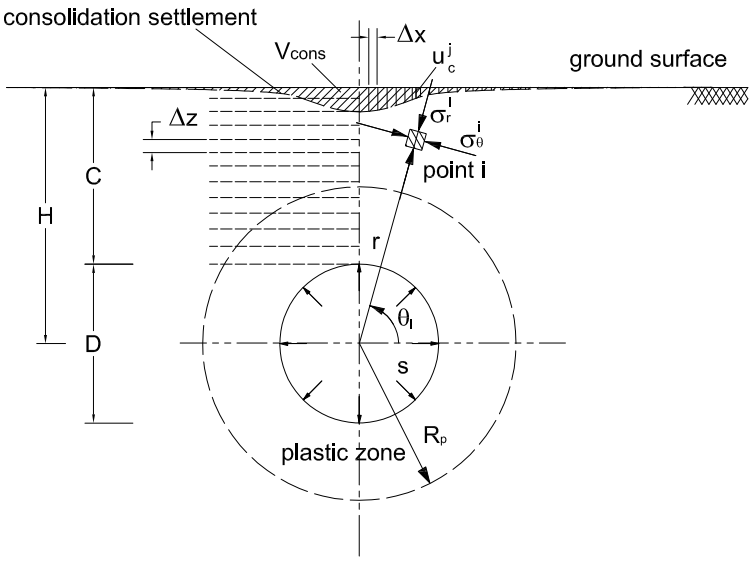

Figure 14: Soil stresses at the tail

where C_s is the compression constant depending on soil type (as can be seen in Table 1), σ_{soil} is the vertical stress in the soil and σ_0 is the initial vertical stress in the soil.
In case the vertical stress is lower than the initial vertical stress, unloading occurs and Equation 16 would be modified to:

$$u_c = -\frac{1}{C_{swel}} \ln\left(\frac{\sigma_{soil}}{\sigma_0}\right) \tag{17}$$

where C_{swel} is the swelling constant depending on soil type (as can be seen in Table 1).
The stress in the soil σ_{soil} is estimated from the radial and tangential stresses derived by the cavity expansion theory as can be seen in Figure 14. According to Yu (2013), the stresses in the elastic zone are given by:

$$\sigma_r = -p_0 + \frac{kY}{1+k}\left(\frac{R_p}{r}\right)^{(1+k)} \tag{18}$$

$$\sigma_\theta = -p_0 - \frac{Y}{1+k}\left(\frac{R_p}{r}\right)^{(1+k)} \tag{19}$$

where σ_r and σ_θ are the radial and tangential stresses as shown in Figure 14. In the plastic zone, the stresses are given by:

$$\sigma_r = -p_0 + \frac{kY}{1+k} + kY \ln \frac{R_p}{r} \tag{20}$$

$$\sigma_\theta = -p_0 - \frac{Y}{1+k} + kY \ln \frac{R_p}{r} \tag{21}$$

In order to estimate the consolidation settlement, the soil volume above the tunnel lining is divided into n layers. The final consolidation settlement is derived by summing deformations of these layers, which are calculated by Equations 16 and 17.
The final consolidation settlement is given by:

$$u_c^j = \sum_{i=1}^{n} u_c^{(j,i)} \Delta z \tag{22}$$

where $u_c^{(j,i)}$ and $\Delta z^{(i)}$ are the deformation due to consolidation and the depth of the i^{th} layer at the j^{th} location along the surface.
Figure 15 shows settlement troughs in the case of tunnelling in clay with a diameter $D = 10m$ and the ratio of $C/D = 1$, as an example. It can be seen that a heave and a settlement can occur depending on what particular support pressure is applied.
By integrating the final consolidation settlements over the surface, the volume of consolidation settlement at the surface V_{cons} can be estimated as:

$$V_{cons} = \sum_{j=1}^{m} u_c^{(j)} \Delta x \tag{23}$$

where Δx is a length increment along the surface consolidation settlement and m is the increment number.
The volume loss due to consolidation settlement is then estimated as:

$$V_{L,c} = \frac{V_{cons}}{\pi (D/2)^2} \tag{24}$$

Figure 16 shows the relationship between the consolidation volume loss $V_{L,c}$ and the C/D ratio for tunnels with different diameters in clay, organic clay and peat. With $0.4 \leq C/D \leq 1.3$ in the case of tunnelling in clay and

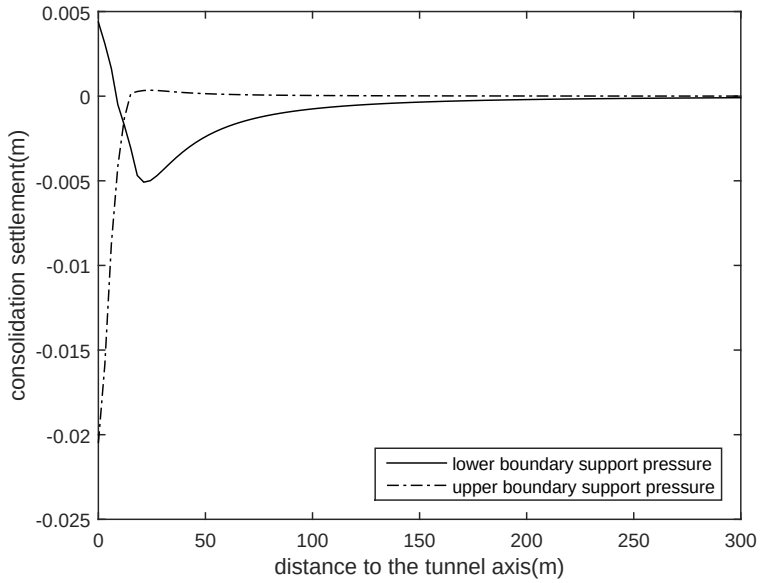

Figure 15: Consolidation settlement troughs when tunnelling in clay with $D = 10m$ and $C/D = 1$

$0.4 \leq C/D \leq 1.7$ in the case of tunnelling in organic clay, it can be seen that the maximum support pressure applied at the tail can lead to a heave on the surface. The volume loss due to consolidation $V_{L,c}$ when maximum support pressure is applied becomes smaller than when minimum support pressure is applied. An example shown in Figure 15 shows that the volume of consolidation settlement V_{cons} when applying lower boundary of support pressure is smaller than the value of V_{cons} when applying the maximum support pressure. When the tunnel is located at a deeper level, the volume loss $V_{L,c}$ when applying the maximum support pressure is higher than the volume loss $V_{L,c}$ in the case of applying minimum support pressure.
The dependence of the volume loss due to consolidation $V_{L,c}$ on soil type is shown in Figure 17 for tunnels with diameters $D = 6$, 8, and $10m$. It can be seen that the volume loss $V_{L,c}$ in the case of tunnelling in peat is much higher compared to tunnelling in clay and organic clay.

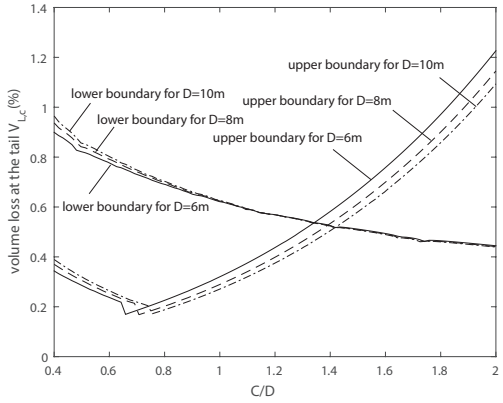

(a) in clay

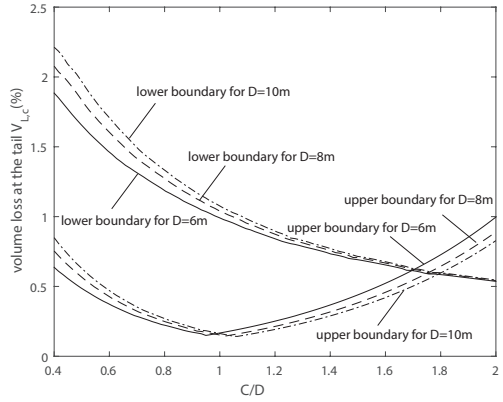

(b) in organic clay

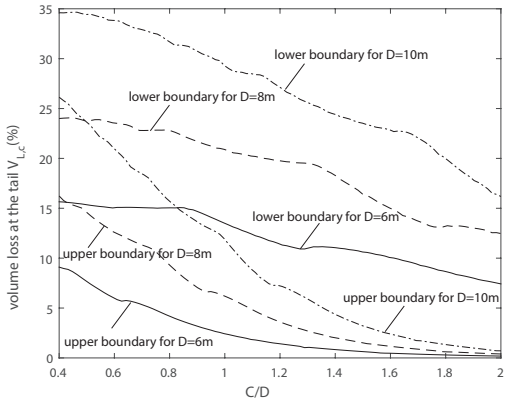

(c) in peat

Figure 16: Volume loss due to consolidation $V_{L,c}$ with different tunnel diameters in various soils

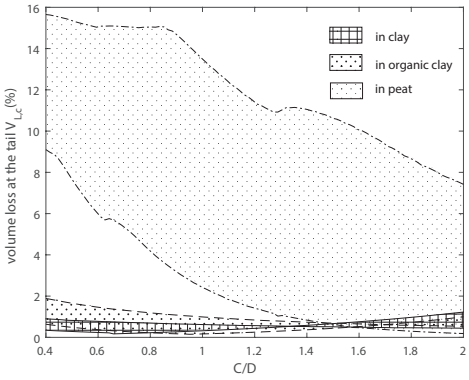

(a) $D = 6m$

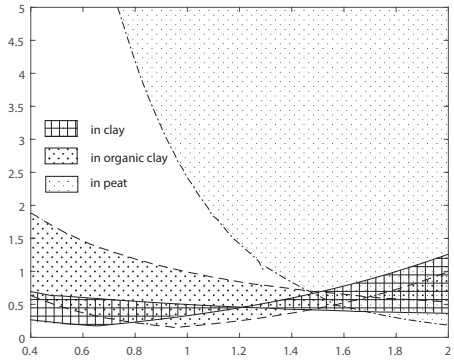

(b) $D = 6m$ (in detailed)

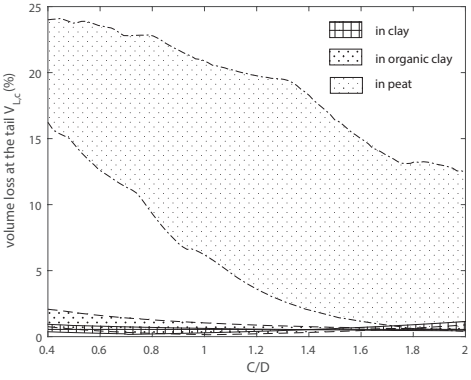

(c) $D = 8m$

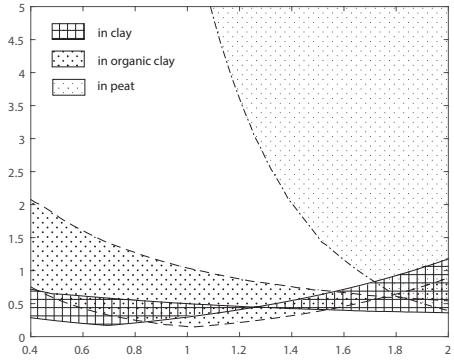

(d) $D = 8m$ (in detailed)

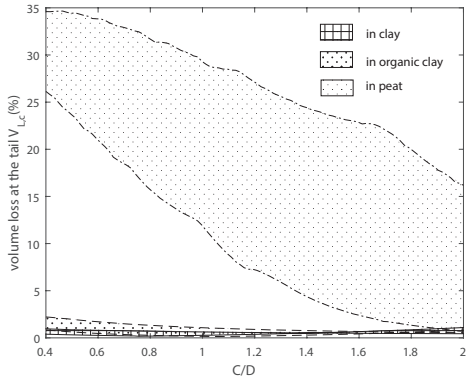

(e) $D = 10m$

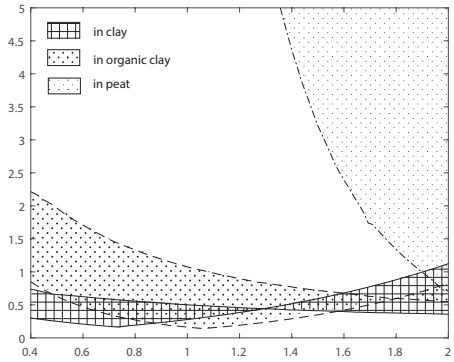

(f) $D = 10m$ (in detailed)

Figure 17: Volume loss due to consolidation $V_{L,c}$ with various tunnel diameters

5. Total volume loss and case studies

5.1. Total volume loss

From Equation 1, the total volume loss is derived by summing the volume loss of tunnelling face, along the shield, at the tail and due to consolidation. Figures 18 and 19 show the total volume loss in the case of shallow tunnelling in sand and clayey sand. It can be seen that the range of the total volume loss decreases with the increase of the C/D ratio and the tunnel diameter D. In the case of a C/D ratio from 0.4 to 1, a volume loss in shallow tunnelling of less than 0.5% can be achieved with the condition of careful monitoring. The highest expected volume loss in this range of the C/D ratio is about 3.7% for tunnelling in sand and 5% for tunnelling in clayey sand when less optimal but still stable support and grout pressures are applied. When the C/D ratio larger than 1, the maximum volume loss is less than 1.5% with the range of support pressures in this study. These figures also show that a result of no volume loss can be achieved when tunnelling with $C/D \geq 2$. Figure 20 shows the relationship between the total volume loss V_L and C/D

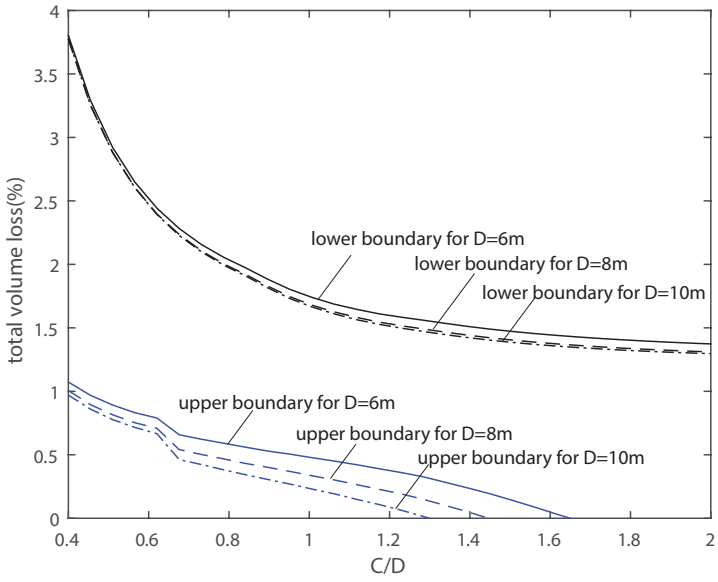

Figure 18: Total volume loss for tunnelling in sand with various diameter D

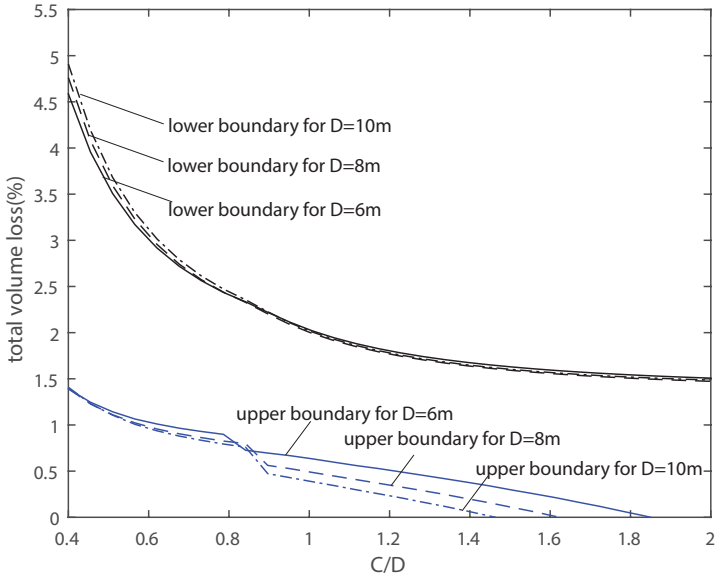

Figure 19: Total volume loss for tunnelling in clayey sand with various diameter D

ratios when tunnelling in clay. The total volume loss V_L when tunnelling has just finished (not taking into account the consolidation) is shown in Figure 20a. It can be seen that a total volume loss V_L less than 0.5% after tunnelling is feasible even with $C/D \leq 1$. This figure also shows that for very shallow tunnelling with $C/D \leq 0.6$, a tunnel with a large diameter has a larger range of expected volume loss. With deeper tunnelling when $1 \leq C/D \leq 2$, the maximum value of the total volume loss reduces and becomes less than 2%.

Figure 20b shows the total volume loss V_L for tunnelling with various diameters $D = 6, 8$ and $10m$ in clay including consolidation of soil layers above the tunnel. It also follows that the lower the C/D ratio is, the larger the range of volume loss is. The total volume loss of tunnelling in clay would be at maximum about 6% with $D = 10m$, 5.5% with $D = 8m$ and 5% with $D = 6m$ when $C/D = 0.4$. The lower boundary corresponding with the minimum support pressure applied has a reducing trend when the C/D ratio increases. This means there might be a larger volume loss when the tunnel becomes shallower. At the upper boundary of the total volume loss, corresponding with the maximum support pressure applied, the final volume loss

of tunnelling with $D = 6m$ can reach just over 0% after consolidation has been taken into account.

5.2. Case studies

Tables 3 and 4 show a summary of volume loss in case histories for tunnelling in sand and clay with the C/D ratio less than 2. In Table 3, there are two case studies the Ayshire Joint Drainage Scheme and WNTDC Lumb Brook Sewer, derived from the study of O'Reilly and New (1982) and three case studies Second Heinenoord Tunnel, Botlek Railway Tunnel and Sophia Railway Tunnel, derived from Netzel (2009). Table 4 shows volume loss data from various projects all over the world including Madrid Metro Extension, Heathrow Express Trail Tunnel, Waterloo, Garrison Dam test tunnel, Baulos 25, Barcelona Subway and London Transport Experimental Tunnel.
The data in Table 3 are plotted in Figure 21a in order to compare the volume loss derived from this analysis to field data in the case of shallow to medium deep tunnelling in sand. It can be seen that most of field data falls in the boundaries of volume loss in Figure 21a.
Figure 21b shows the validation of the calculated volume loss to the field data in Table 4 in the case of shallow tunnelling in clay. It also shows that all the field data is in agreement with the boundaries of volume loss derived in this study. Only the Madrid Metro Extension which is known as a successful tunnelling project has one data point below the lower boundary of volume loss for a low C/D ratio.
The agreement between derived boundaries of volume loss in sand and clay and field data shows that the approach of estimating volume loss in this study can successfully predict volume loss in shallow tunnelling.

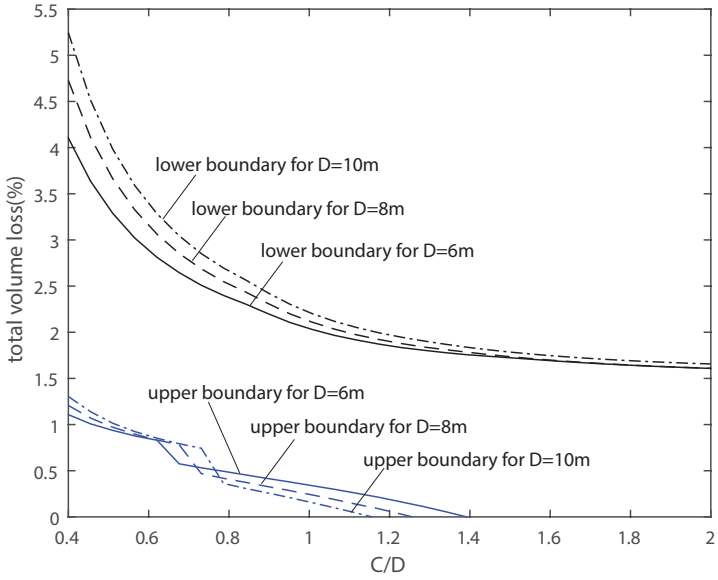

(a) not including consolidation of soil layers above the tunnel

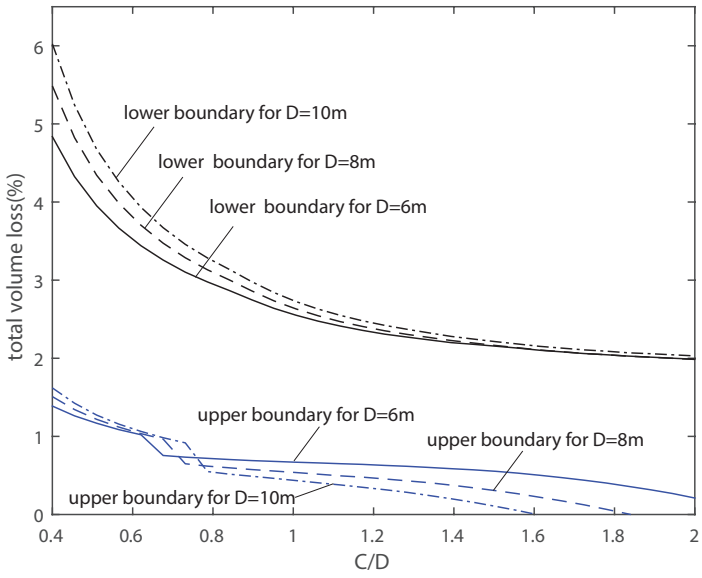

(b) including consolidation of soil layers above the tunnel

Figure 20: Total volume loss for tunnelling in clay with various diameter D

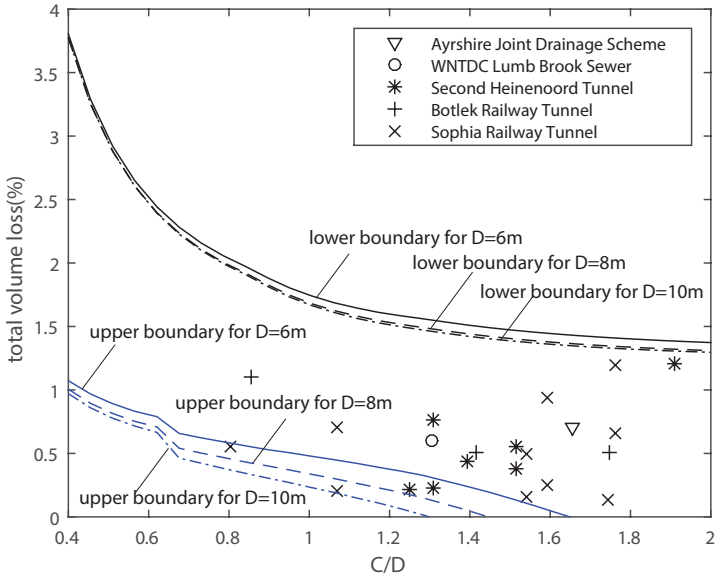

(a) in sand

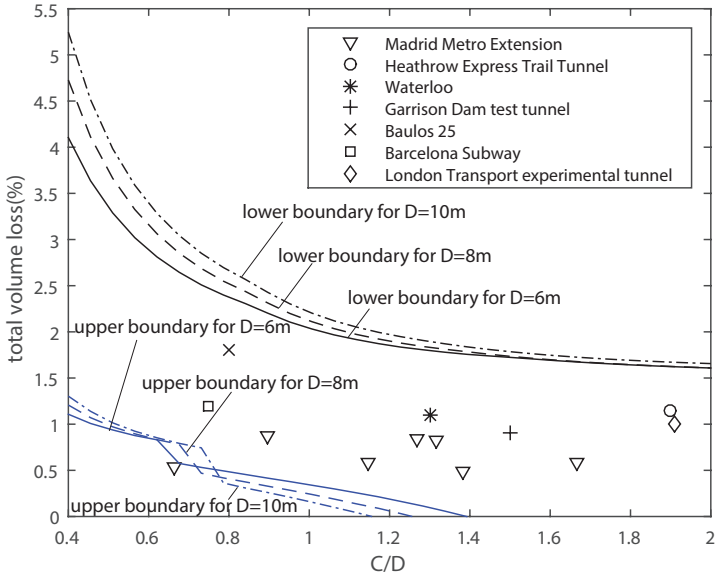

(b) in clay

Figure 21: Validation for volume loss in shallow tunnelling

Case	H(m)	C(m)	D(m)	C/D	V_L(%)	Soil conditions	Reference
Ayrshire Joint Drainage Scheme	6.25	4.8	2.9	1.66	0.7	fine to medium slightly silty sand; loose and medium density	O'Reilly and New (1982)
WNTDC Lumb Brook Sewer	6.5	4.7	3.6	1.31	0.5	medium/dense sands and gravel with a little clay	O'Reilly and New (1982)
Second Heinenoord Tunnel	14.5	10.37	8.3	1.25	0.21	dense sand	Netzel (2009)
	15.0	10.8	8.3	1.31	0.22		
	15.0	10.8	8.3	1.31	0.7		
	15.7	11.6	8.3	1.39	0.44		
	16.7	12.6	8.3	1.51	0.38		
	16.7	12.6	8.3	1.51	0.55		
	20.0	15.8	8.3	1.91	1.2		
Botlek Railway Tunnel	13.1	8.3	9.65	0.86	1.11	Holoceen and Pleistoceen sand	Netzel (2009)
	18.5	13.7	9.65	1.42	0.5		
	21.7	16.9	9.65	1.75	0.5		
Sophia Railway Tunnel	12.4	7.6	9.5	0.8	0.55	Pleistoceen sand	Netzel (2009)
	14.9	10.1	9.5	1.1	0.21		
	14.9	10.1	9.5	1.1	0.7		
	19.4	14.7	9.5	1.5	0.15		
	19.4	14.7	9.5	1.5	0.5		
	19.9	15.1	9.5	1.6	0.25		
	19.9	15.1	9.5	1.6	0.94		
	21.3	16.6	9.5	1.7	0.14		
	21.5	16.75	9.5	1.8	0.65		
	21.5	16.75	9.5	1.8	1.2		

Table 3: Volume loss of tunnelling in sand projects

Case	H(m)	C(m)	D(m)	C/D	V_L(%)	Soil conditions	Reference
Madrid Metro Extension	10.3	5.9	8.88	0.66	0.54	stiff clay	Melis et al. (2002)
	12.43	8	8.88	0.9	0.87		
	14.61	10.17	8.88	1.15	0.6		
	15.7	11.26	8.88	1.27	0.84		
	16.12	11.68	8.88	1.32	0.83		
	16.7	12.27	8.88	1.38	0.5		
	19.23	14.79	8.88	1.67	0.58		
Heathrow Express Trail Tunnel	21	16.67	8.66	1.9	1.15	London clay	Bowers et al. (1996)
Waterloo	11.7	8.45	6.5	1.3	1.1	London clay	Harris et al. (1994)
Garrison Dam Test Tunnel	11	8.25	5.5	1.5	0.9	clay-shale and lignite	Peck (1969)
Baulos 25	8.45	5.2	6.5	0.8	1.8	Frankfurt clay	Macklin (1999)
Barcelona Subway	10	6	8	0.75	1.2	red and brown clay with some gravel	Ledesma and Romero (1997)
London Transport Experimental Tunnel	10	7.9	4.15	1.91	1	dense sandy gravel overlain with made ground of soft clay with sand and gravel	O'Reilly and New (1982)

Table 4: Volume loss of tunnelling in clay projects

6. Conclusion

Volume loss is a major parameter in the calculation of ground movement by tunnelling. The range of attainable volume loss can be estimated by combining stability analysis at tunnelling face, along and behind the shield. In this theoretical study, it is found that in the case of tunnelling with $C/D \leq 1$, the volume loss at the tunnelling face has a major impact in total volume loss.

The volume loss along the shield can be optimized by selecting optimal bentonite and grout pressures applied at tunnelling face and tail. The proposed calculation method estimates attainable upper and lower boundaries of volume loss along the shield for a particular tunnel.

This paper also presents methods to identify the volume loss behind the shield. The volume loss at the tail when tunnelling in peat has a large impact, especially in the case of shallow tunnels ($C/D \leq 1$). The volume loss behind the tail was estimated by the volume loss due to shrinkage of grout and consolidation of above soil volume. The volume loss due to consolidation depends on the surrounding soil and the C/D ratio.

The total volume losses for tunnelling in sand, clayey sand and clay are derived and have a good agreement with case studies. Overall, the range of volume loss increases when tunnelling with shallower overburden. By controlling the applied support pressure at the tunnelling face and tail, the volume loss can be minimized. Still, a direct volume loss around 1% is a reasonable minimum for very shallow tunnels ($C/D = 0.4$) where for deeper tunnels no volume loss should be attainable. If pressure control is less optimal but still controlled, a direct volume loss up to 5.5% is not unreasonable to expect for very shallow tunnels.

Analysis also shows that consolidation after the TBM has passed can contribute considerably to the final surface settlements and can be of this same order as direct volume loss effects in clay and even larger in very soft soils like peat. This effect, however, is more pronounced in deeper tunnels, where it could easily double the direct volume loss.

References

Anagnostou, G., Kovári, K., 1994. The face stability of slurry-shield-driven tunnels. Tunnelling and Underground Space Technology 9 (2), 165–174.

Attewell, P., Farmer, I., 1974. Ground disturbance caused by shield tunnelling in a stiff, overconsolidated clay. Engineering Geology 8 (4), 361–381.

Attewell, P. B., Yeates, J., Selby, A. R., 1986. Soil movements induced by tunnelling and their effects on pipelines and structures. Methuen, Inc., New York, NY.

Bezuijen, A., 2007. Bentonite and grout flow around a tbm. In: Underground Space–The 4th Dimension of Metropolises, Three Volume Set+ CD-ROM: Proceedings of the World Tunnel Congress 2007 and 33rd ITA/AITES Annual General Assembly, Prague, May 2007. CRC Press, p. 383.

Bezuijen, A., Talmon, A., 2008. Processes around a tbm. In: Proceedings of the 6th International Symposium on Geotechnical Aspects of Underground Construction in Soft Ground (IS-Shanghai 2008). pp. 10–12.

Bezuijen, A., Talmon, A., 2013. Grout properties and their influence on back fill grouting. In: Proceedings of the 5th International Symposium on Geotechnical Aspects of Underground Construction in Soft Ground. p. 187.

Bosch, J. W., Broere, W., 2009. Small incidents, big consequences. leakage of a building pit causes major settlement of adjacent historical houses. amsterdam north-south metro line project. In: Safe Tunnelling for the City and Environment: ITA-AITES World Tunnel Congress, 23-28 May 2009, Budapest, Hungary. Hungarian Tunneling Association.

Bowers, K., Hiller, D., New, B., 1996. Ground movement over three years at the heathrow express trial tunnel. In: Proceedings of the international symposium on geotechnical aspects of underground construction in soft ground, London. pp. 557–562.

Broere, W., 2001. Tunnel face stability & new cpt applications. Ph.D. thesis, Delft University of Technology.

Broms, B. B., Bennermark, H., 1967. Stability of clay at vertical openings. Journal of Soil Mechanics & Foundations Div.

Cording, E. J., Hansmire, W., 1975. Displacements around soft ground tunnels. In: 5th Pan American Congress on Soil Mechanics and Foundation Engineering. Vol. 4. Buenos Aires, pp. 571–633.

Dimmock, P. S., Mair, R. J., 2007. Estimating volume loss for open-face tunnels in london clay. Proceedings of the ICE-Geotechnical Engineering 160 (1), 13–22.

Festa, D., Broere, W., Bosch, J., 2015. Kinematic behaviour of a tunnel boring machine in soft soil: Theory and observations. Tunnelling and Underground Space Technology 49, 208–217.

Gemeente-Amsterdam, 2009. Geotechnical base report alternative design deep stations and risk assessment bored tunnel. Tech. rep., Projectbureau Noord/Zuidlijn.

Harris, D., Mair, R., Love, J., Taylor, R., Henderson, T., 1994. Observations of ground and structure movements for compensation grouting during tunnel construction at waterloo station. Geotechnique 44 (4), 691–713.

Jancsecz, S., Steiner, W., 1994. Face support for a large mix-shield in heterogeneous ground conditions. In: Tunnelling94. Springer, pp. 531–550.

Ledesma, A., Romero, E., 1997. Systematic backanalysis in tunnel excavation problems as a monitoring technique. In: Proceedings of the International Conference on Soil Mechanics and Foundation Engineering- International Society for Soil Mechanics and Foundation Engineering. Vol. 3. AA BALKEMA, pp. 1425–1428.

Loganathan, N., 2011. An innovative method for assessing tunnelling-induced risks to adjacent structures. New York: Parsons Brinckerhoff Inc. One Penn Plaza New York.

Macklin, S., 1999. The prediction of volume loss due to tunnelling in overconsolidated clay based on heading geometry and stability number. Ground engineering 32 (4), 30–33.

Mair, R., 1989. Discussion leaders report on session 9: Selection of design parameters for underground construction. In: Proceedings of the 12th International Conference on Soil Mechanics and Foundation Engineering, Rio de. Vol. 5. pp. 2891–2893.

Mair, R., Gunn, M., O'REILLY, M., 1982. Ground movement around shallow tunnels in soft clay. Tunnels & Tunnelling International 14 (5).

Mair, R., Taylor, R., 1999. Theme lecture: Bored tunnelling in the urban environment. of XIV ICSMFE [131], 2353–2385.

Mair, R., Taylor, R., Bracegirdle, A., 1993. Subsurface settlement profiles above tunnels in clays. Geotechnique 43 (2).

Melis, M., Medina, L., Rodríguez, J. M., 2002. Prediction and analysis of subsidence induced by shield tunnelling in the madrid metro extension. Canadian Geotechnical Journal 39 (6), 1273–1287.

Mori, A., Tamura, M., Kurihara, K., Shibata, H., 1991. A suitable slurry pressure in slurry-type shield tunneling. Proc Tunnelling '91, London, 361–369.

Nagel, F., Meschke, G., 2011. Grout and bentonite flow around a tbm: Computational modeling and simulation-based assessment of influence on surface settlements. Tunnelling and Underground Space Technology 26 (3), 445–452.

NEN-3650, 2012. NEN 3650-2012 nl Eisen voor buisleidingsystemen.

Netzel, H. D., 2009. Building response due to ground movements. TU Delft, Delft University of Technology.

O'Reilly, M., 1988. Evaluating and predicting ground settlements caused by tunnelling in london clay. In: Tunnelling. Vol. 88. pp. 231–241.

O'Reilly, M., New, B., 1982. Settlements above tunnels in the united kingdom-their magnitude and prediction. Tech. rep., Institution of Mining and Metallurgy.

Peck, R. B., 1969. Deep excavations and tunnelling in soft ground. In: Proc. 7th Int. Conf. on SMFE. pp. 225–290.

Sagaseta, C., 1988. Analysis of undrained soil deformation due to ground loss. Geotechnique 38 (4).

Strack, O. E., 2002. Analytic solutions of elastic tunneling problems. Ph.D. thesis, Delft University of Technology.

Talmon, A., Bezuijen, A., 2009. Simulating the consolidation of tbm grout at noordplaspolder. Tunnelling and Underground Space Technology 24 (5), 493–499.

Taylor, R., R., 1993. Prediction of clay behaviour around tunnels using plasticity solutions. In: Predictive Soil Mechanics: Proceedings of the Wroth Memorial Symposium Held at St. Catherine's College, Oxford, 27-29 July 1992. Thomas Telford, p. 449.

Verruijt, A., 1997. A complex variable solution for a deforming circular tunnel in an elastic half-plane. International Journal for Numerical and Analytical Methods in Geomechanics 21 (2), 77–89.

Verruijt, A., Booker, J., 1996. Surface settlements due to deformation of a tunnel in an elastic half plane. Geotechnique 46 (4), 753–756.

Vu, M. N., Broere, W., Bosch, J. W., 2015a. Effects of cover depth on ground movements induced by shallow tunnelling. Tunnelling and Underground Space Technology 50, 499–506.

Vu, M. N., Broere, W., Bosch, J. W., 2015b. The impact of shallow cover on stability when tunnelling in soft soils. Tunnelling and Underground Space Technology 50, 507–515.

Yu, H.-S., 2013. Cavity expansion methods in geomechanics. Springer Science & Business Media.